Acta Crystallographica Section D
Biological Crystallography
ISSN 0907-4449

Coiled-coil conformation of a pentamidine–DNA complex

Tadeo Moreno,[a] Joan Pous,[b] Juan A. Subirana[a]* and J. Lourdes Campos[a]*

[a]Departament d'Enginyeria Química, Universitat Politècnica de Catalunya, E-08028 Barcelona, Spain, and [b]Plataforma Automatitzada de Cristallografia, IRB–PCB–CSIC, E-08028 Barcelona, Spain

Correspondence e-mail: juan.a.subirana@upc.edu, lourdes.campos@upc.edu

Received 6 November 2009
Accepted 29 December 2009

PDB Reference: pentamidine–DNA complex, 3ey0.

NDB Reference: DD0102.

The coiled-coil structure formed by the complex of the DNA duplex d(ATATATATAT)$_2$ with pentamidine is presented. The duplex was found to have a mixed structure containing Watson–Crick and Hoogsteen base pairs. The drug stabilizes the coiled coil through the formation of cross-links between neighbouring duplexes. The central part of the drug is found in the minor groove as expected, whereas the charged terminal amidine groups protrude and interact with phosphates from neighbouring molecules. The formation of cross-links may be related to the biological effects of pentamidine, which is used as an antiprotozoal agent in trypanosomiasis, leishmaniasis and pneumonias associated with AIDS. The DNA sequence that was used is highly abundant in most eukaryotic genomes. However, very few data are available on DNA sequences which only contain A·T base pairs.

1. Introduction

The fact that alternating AT sequences may form coiled coils (Campos *et al.*, 2005; De Luchi *et al.*, 2006) was the main motivation for our choice of sequence to crystallize. Here, we report that d(ATATATATAT) does indeed form a similar structure, but its detailed features are quite different from those observed previously, as will be shown below. Furthermore, oligonucleotides with an alternating AT sequence often form duplexes containing Hoogsteen base pairs (Abrescia *et al.*, 2002; De Luchi *et al.*, 2006). This conformation of DNA appears to be stabilized by the presence of extrahelical thymine residues in the minor groove (Pous *et al.*, 2008). Therefore, we thought that minor-groove-binding drugs may also stabilize the Hoogsteen conformation of DNA with an alternating AT sequence. With these objectives in mind, here we present the structure of the complex of the oligonucleotide d(ATATATATAT) with pentamidine. We found that in the presence of the drug only one base pair remains in the Hoogsteen conformation. In the region of interaction the duplex has the standard B form of DNA with Watson–Crick base pairs, but the structure of the complex is different from that previously described (Edwards *et al.*, 2003). The terminal charged groups of the drug interact with neighbouring DNA molecules. Thus, the drug acts as a cross-linking agent in the crystal structure. This mode of interaction has not been described for any previously studied minor-groove-binding drugs (Tidwell & Boykin, 2003; Baraldi *et al.*, 2004; Nguyen *et al.*, 2009).

Table 1
Crystal data and refinement statistics.

Values in parentheses are for the last shell.

Wavelength (Å)	0.9795
Temperature (K)	104
Space group	$P6_522$
Unit-cell parameters (Å, °)	$a = b = 27.789$, $c = 311.95$, $\alpha = \beta = 90$, $\gamma = 120$
Resolution range (Å)	50–2.52 (2.56–2.52)
Unique reflections	2899 (128)
Free *R*-factor reflections	262
Completeness (%)	94.7 (100.0)
Redundancy factor	15.8 (18.4)
$\langle I/\sigma(I)\rangle$	37.6 (15.7)
$R_{\rm merge}$†	0.098 (0.212)
Contents of asymmetric unit	
DNA duplexes	1
Pentamidines	1
Magnesiums	1
Water molecules	51
Total non-H atoms	481
$R_{\rm work}$‡	0.216 (0.248)
$R_{\rm free}$§	0.277 (0.411)
Mean *B* factor (Å^2)	43.5
R.m.s.d. bonds (Å)	0.018
R.m.s.d. angles (°)	1.64
R.m.s.d. chiral (Å^3)	0.052

† $R_{\rm merge}(I) = \sum_{hkl}\sum_i |I_i(hkl) - \langle I(hkl)\rangle|/\sum_{hkl}\sum_i I_i(hkl)$ calculated for the whole data set. ‡ $R_{\rm work} = \sum_{hkl}||F_{\rm obs}| - |F_{\rm calc}||/\sum_{hkl}|F_{\rm obs}|$. § $R_{\rm free}$ is the *R* factor calculated for the reflections used for cross-validation during refinement.

We should also note that the alternating AT sequence is extremely abundant in all organisms (Subirana & Messeguer, 2008). The malaria parasite *Plasmodium falciparum*, for example, has 80.6% AT and contains 396 000 occurrences of the sequence $(AT)_5$ in its 22.9 Mb genome. In the human genome the $(AT)_5$ sequence occurs over a million times. Therefore, the abundant alternating $(AT)_n$ sequences are a likely target for the biological effects of pentamidine and other minor-groove-binding drugs. Thus, the activity of pentamidine against protozoal infections (Baraldi *et al.*, 2004) and mitotic cancer cells (Lee *et al.*, 2007) may arise from interaction with such sequences, although the mechanism of action is not well known (Baraldi *et al.*, 2004). A possible mechanism involves interactions with the AT-rich DNA found in the kinetoplasts of protozoa (Wilson *et al.*, 2008).

2. Materials and methods

2.1. Chemicals

The oligonucleotide d(ATATATATAT) was synthesized in an automatic synthesizer by the phosphoramidite method and was purified by gel filtration and reverse-phase HPLC.

The drug pentamidine [1,5-bis(4-amidinophenoxy)pentane] was bought from Aldrich (439843) as the isethionate salt.

2.2. Crystallization

Crystals were grown by vapour diffusion at 278 K in hanging drops. The drops contained 6.7 m*M* $MgCl_2$, 17 m*M* 2-(*N*-morpholino)ethanesulfonic acid (MES) pH 6.0 and 5% 2-propanol (Natrix condition No. 7; Hampton Research). The concentrations of double-stranded DNA and pentamidine were 0.36 and 2.4 m*M*, respectively, with a total volume of 6 µl. The drops were equilibrated against a reservoir consisting of 15% 2-methyl-2,4-pentanediol (MPD) solution. The MPD concentration was slowly increased to 37%. A constant 5% concentration of 2-propanol was maintained at all times.

Crystals grew as hexagonal columns in seven weeks. Typical crystals were approximately 0.3 × 0.3 × 0.6 mm in size. The crystals were flash-frozen in liquid nitrogen and stored until use.

2.3. Data collection, structure solution and refinement

The crystal was mounted in a loop and kept in a nitrogen-gas stream at 104 K. Diffraction data were collected at a wavelength of 0.9795 Å on an ADSC Quantum-210 detector on the Spanish beamline BM-16 at the ESRF (Grenoble,

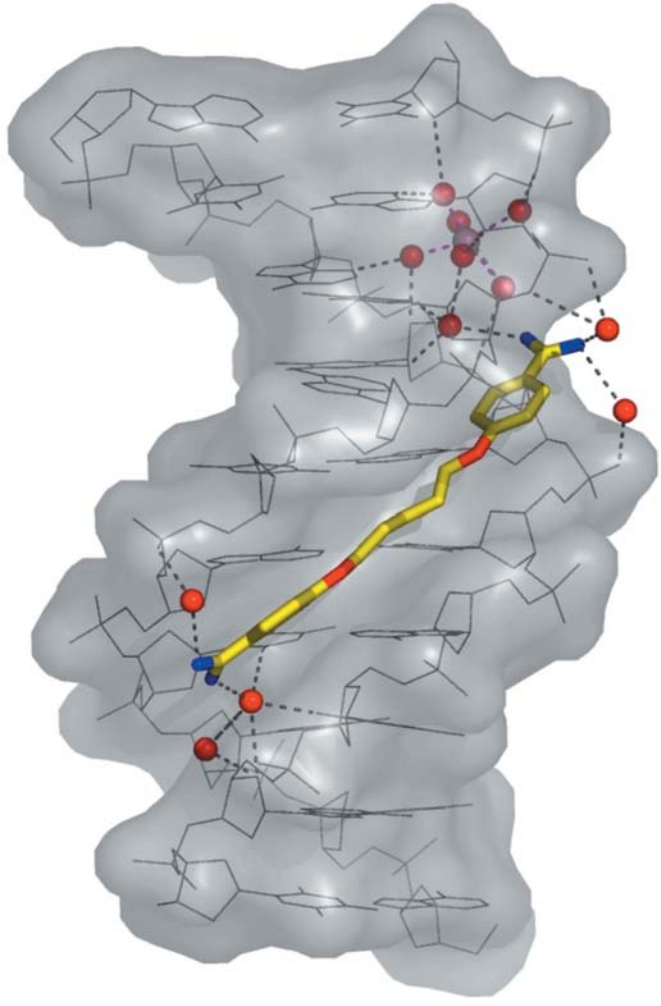

Figure 1
View of the pentamidine–d(ATATATATAT)$_2$ complex. The drug is in the minor groove at the centre of the sequence. The water molecules and one Mg^{2+} ion found in the minor groove are also shown. Hydrogen bonds are represented as dashed lines. The two ends of the duplex are different. At one end (top) the duplex forms standard Watson–Crick base pairs. At the other end (bottom) a Hoogsteen A·T base pair is present. Note that the Mg^{2+} ion is at the back of the duplex in this presentation.

France). Images with an oscillation angle of 2° were collected from 0 to 180° at a maximum resolution of 2.52 Å.

Indexing and data processing were carried out using the *HKL*-2000 (Otwinowski & Minor, 1997) and *CCP*4 (Collaborative Computational Project, Number 4, 1994) program packages. The average mosaicity was 0.24°. The molecules are organized in a hexagonal cell with high symmetry ($P6_522$), with a single oligonucleotide duplex in the asymmetric unit. The structure was solved by molecular replacement with the program *AMoRe* (Navaza, 1994), refined with *REFMAC* (Murshudov *et al.*, 1997) and validated with 3*DNA* (Lu & Olson, 2003).

A Hoogsteen pairing mode was first tried as this conformation had previously been found in alternating AT sequences (Abrescia *et al.*, 2002; De Luchi *et al.*, 2006). However, the structure could not be refined. We then used a standard B-form DNA model and refinement became possible. We also added a pentamidine molecule in a region of high extra density in the minor groove. A hydrated magnesium ion was also added in the minor groove at the Watson–Crick end of the duplex. At this point we obtained an R_{work} of 0.285 and an R_{free} of 0.337, but the electron-density maps of base pairs adenine 9A·thymine 2B and thymine 10A·adenine 1B were not correct. We changed the latter base pair to the Hoogsteen conformation and the R values fell to 0.253 and 0.323, respectively. The electron-density map of this base pair was then very good, as will be shown below. On the other hand, the electron-density map of the next base pair 9A·2B was unusual. We tried to model this base pair with partial occupancy of Watson–Crick and Hoogsteen conformations without success. The conformation of this base pair is probably influenced by its being adjacent to a Hoogsteen base pair. A reasonable electron-density map was finally obtained after several cycles of refinement. Nevertheless, it is likely that some contribution from partial occupancy of a Hoogsteen conformation contributes to the electron density in this region, since the C1′—C1′ distance (9.8 Å) is somewhat smaller than the standard value for Watson–Crick base pairing (10.5 Å). Higher resolution data are required in order to model this base pair with greater precision.

Refinement was continued by adding water molecules, with final values of R_{work} = 0.216 and R_{free} = 0.277. Crystal data and refinement statistics are given in Table 1. Figures were produced with *Cerius*2 (Accelrys Inc.) and *PyMOL* (http://www.pymol.org).

Disorder in the 9A·2B base pair could also be a consequence of twinning. The crystals might have a lower symmetry and be merohedrally twinned with two decamers in the asymmetric unit. However, when we calculated the cumulative intensity distribution using the *TRUNCATE* program from the *CCP*4 suite we did not find any signs of twinning. Moreover, the refinement progressed smoothly to final reasonably low R values. It neither became stuck at high R values nor generated a map of unrelated quality to the R values.

3. Results

3.1. Pentamidine interactions

The structure of the complex of pentamidine with the DNA duplex is shown in Fig. 1. The drug is placed in the centre, so that the hydrophobic methylene groups and benzene rings are tightly bound to the minor groove, but no hydrogen bonds are

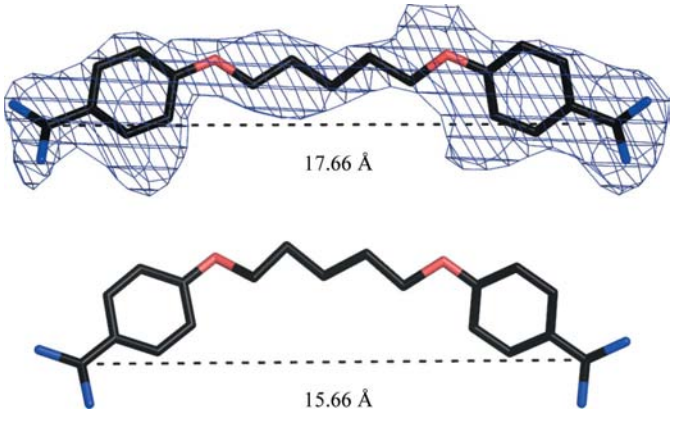

Figure 2
Comparison of the structures of the pentamidine drug associated with either d(ATATATATAT)$_2$ (top) or d(CGCGAATTCGCG)$_2$ (bottom; Edwards *et al.*, 2003). The electron-density map ($2F_o - F_c$ at the 1σ level) is shown for the former, which is more stretched than that found in the latter. The distance between the amidino C atoms is indicated.

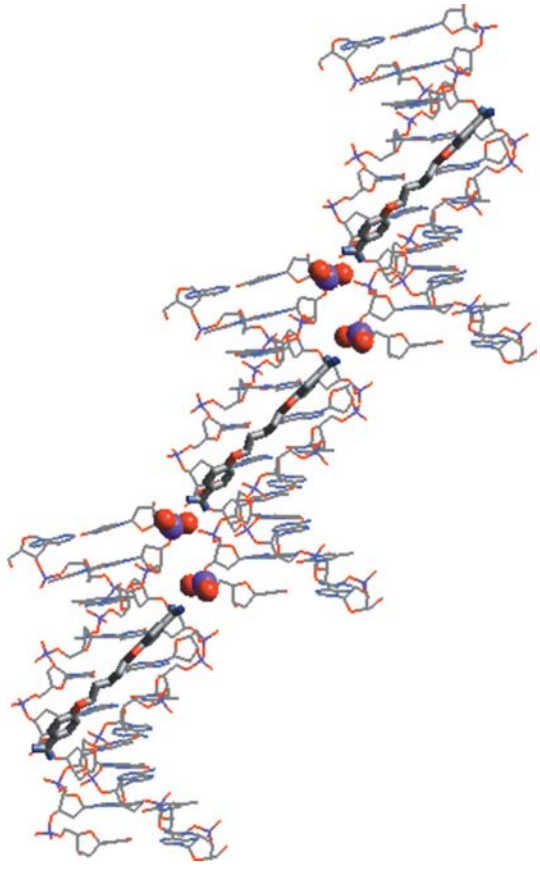

Figure 3
The charged terminal groups of the drug interact with the phosphates of neighbouring duplexes in the crystal. Phosphates are shown as spheres.

possible. When the drug enters the minor groove it displaces most of the water molecules present in the groove that have been described in other alternating AT sequences (Yuan *et al.*, 1992). As demonstrated by Chaires (1997), the main stabilizing force of drugs in the minor groove of DNA arises from removal of the hydrophobic regions from contact with the solvent; hydrogen bonds are not required.

The positively charged terminal amidine groups of the drug interact with the DNA bases *via* hydrogen-bonded waters. The water molecules act as a bridge between the DNA bases and pentamidine. One fully hydrated Mg^{2+} ion is also present in the minor groove at one end of the duplex, as shown in Fig. 1. In general, the drug appears to interact with DNA in a manner similar to that described in previous studies of drug–DNA complexes (Fig. 2), although the drug is significantly more stretched than is found when it is bound to d(CGCGAATTCGCG)$_2$ (Edwards *et al.*, 2003). In the latter case the drug is bent and follows the curvature of the minor groove more closely. The terminal amidine N atoms form direct hydrogen bonds to adenines and cytosines.

The main difference between the structure reported here and those of other drug–DNA complexes is the interaction with neighbouring molecules. The terminal amidine groups protrude from the duplex and interact with phosphates in neighbouring duplexes, as shown in Fig. 3. The drug forms electrostatic hydrogen bonds to the thymine 10A phosphate at one end and the thymine 10B phosphate at the other end. The oxygen–nitrogen distances are in the range 2.7–3.1 Å. Note that in another drug related to pentamidine, which has a straight conformation (Nguyen *et al.*, 2002), the drug also binds inside the minor groove of d(CGCGAATTCGCG)$_2$ but does not interact with neighbouring DNA molecules.

3.2. Geometry of the decamer duplex

In spite of the apparent symmetry of the oligonucleotide duplex, its two ends are significantly different. At one end the base pairs are of the normal Watson–Crick type, as found in the central region where the drug is placed. At the other end a clear Hoogsteen base pair is found. The next base pair has an unusual electron-density map: it appears to have an additional hydrogen bond between the O2 atom of thymine and the C2 atom of adenine (the C—O distance is 3.02 Å). Such a hydrogen bond has been suggested to be present in nucleic acid base pairs (Leonard *et al.*, 1995), but the C—O distance observed here is significantly shorter than the previously reported values of around 3.4 Å. This unusual feature might be a consequence of the fact that this base pair is sandwiched between Hoogsteen and standard Watson–Crick base pairs. However, as discussed in §2 the apparent electron-density map is probably due to local disorder arising from a mixture of Hoogsteen and Watson–Crick base pairs at this position. Electron-density maps of the three types of base pairs found in this structure are presented in Fig. 4.

The conformational features of the duplex were calculated with 3*DNA* (Lu & Olson, 2003) and normal parameters were found as in other alternating AT sequences (Abrescia, Malinina, Fernandez *et al.*, 1999). All base pairs show a negative propeller twist in the range −6° to −15.8°. As expected, the AT base steps have a low twist (average 32.0°), whereas the TA base steps have a high twist (average 41.0°). The minor groove is moderately narrow and has a rather uniform width (4.2 Å after subtraction of the van der Waals radii of the phosphates).

3.3. The coiled coil

In the crystal the oligonucleotide duplexes are stacked end to end and give rise to a left-handed coiled coil with hexagonal symmetry, as shown in Figs. 5 and 6: a pseudo-continuous coiled double helix is formed. The duplexes are organized head to head and tail to tail, as shown schematically in Fig. 5(*a*). Thus, the Hoogsteen end of each duplex is in contact with the same end of its neighbouring duplex. The Watson–Crick ends are also in contact. The dyads of the $P6_522$ space group are found at both ends of each duplex. The coiled coils are tightly packed, like a bundle of twisted spaghetti. In the crystal each coiled coil is surrounded by six other identical coiled coils and interacts with all of them through phosphate–pentamidine ionic bonds, as shown in Fig. 3. The diameter of the coiled coils is 85 Å, as measured from the centre of mass of the duplexes; the pitch is 312 Å, with 12 duplexes in a helical turn.

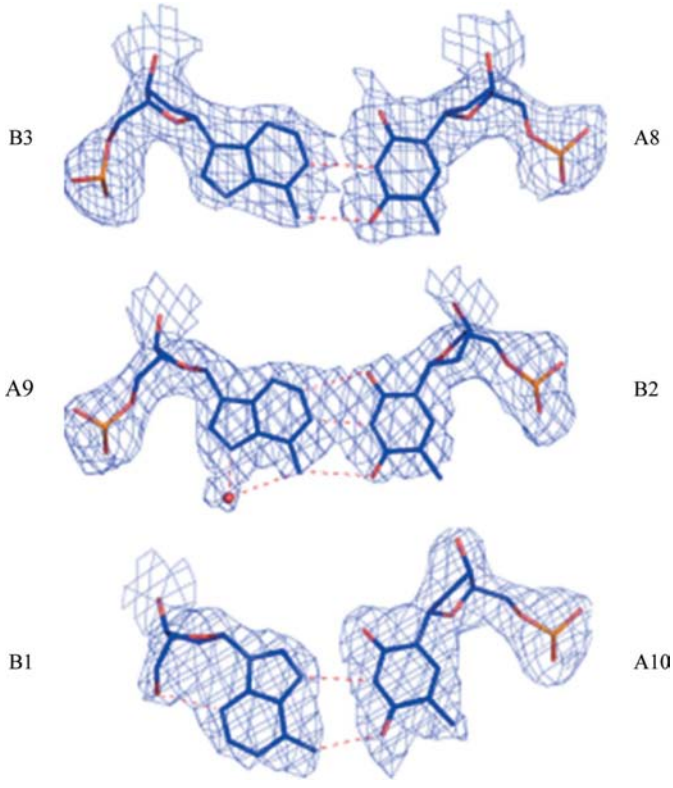

Figure 4
Electron-density maps ($2F_o - F_c$ at the 1σ level) of the Hoogsteen base pair A10·B1, the distorted Watson–Crick base pair B2·A9 and a standard Watson–Crick base pair (A8·B3). The bases are designed by their code in the PDB file. A water molecule is shown as a sphere. Hydrogen bonds are indicated as dashed lines. All of them are in the range 2.7–3.1 Å.

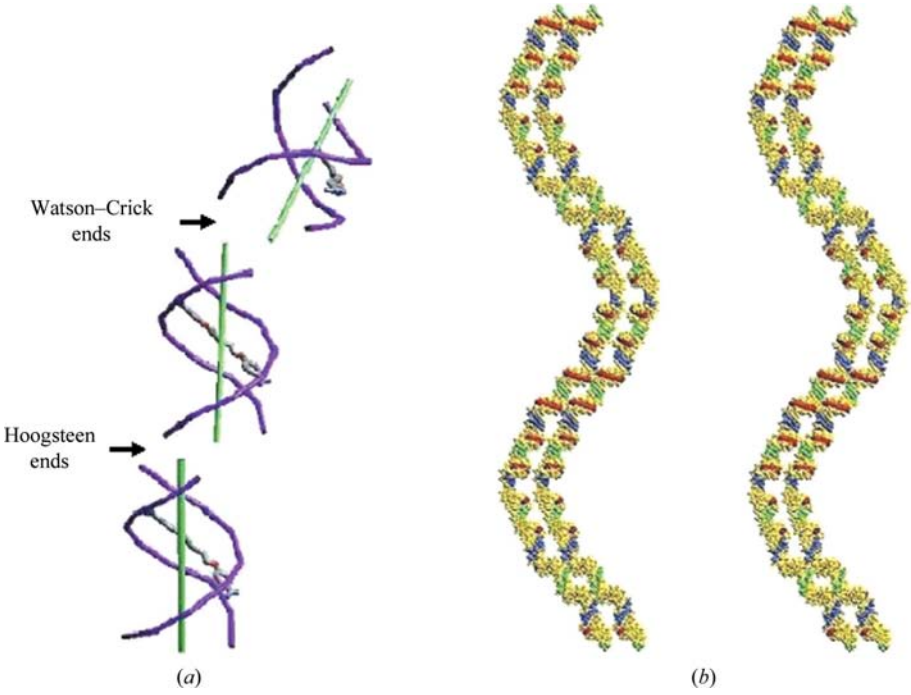

Figure 5
Overall features of the left-handed coiled-coil structure. (*a*) Simplified view of three consecutive duplexes which are part of the same coiled coil. DNA bases are not shown. In the phosphodiester backbone only the phosphate atoms (magenta) are shown with virtual bonds between them. The axis of each duplex calculated with 3*DNA* is presented in green. The drug is also shown. (*b*) Stereoview of one and a half turns of the coiled-coil structure. The drug is shown in red, the terminal Hoogsteen base pair in green and the Watson–Crick base pair at the opposite end in blue. Only two neighbouring coiled coils are shown.

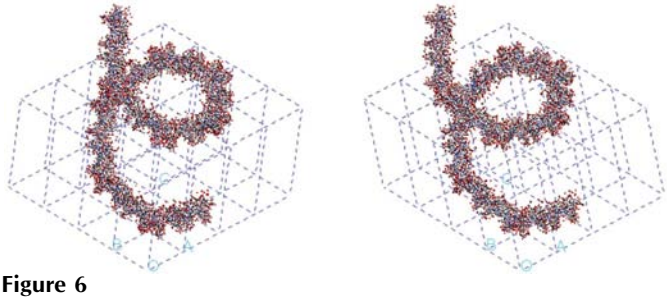

Figure 6
Stereo pair showing a perspective view of one and a half turns of the coiled coil. Each individual coiled coil runs through several unit cells of the crystal. The borders between the 16 unit cells in the drawing are also shown by dashed lines.

The interactions between the Hoogsteen ends generate a pseudo-continuous straight DNA helix, but with a large shift (of about 9 Å) between the terminal Hoogsteen base pairs (B1·A10) of the two helices in contact. There is partial base stacking of adenines and thymines, as shown in Fig. 7. The twist angle between the two base pairs, calculated from the C1′–C1′ angle, is 47°. This value is practically identical to that found in the Hoogsteen structure of d(ATATAT) (Abrescia *et al.*, 2002).

At the Watson–Crick end the duplexes are also shifted and a sharp kink of 37.1° is present, which is the main determinant of the coiled-coil (or kinked-coil) geometry of the stack of duplexes. The base pairs are displaced so that there is optimal stacking between adenines. Thymines are stacked onto the sugar ring of the neighbouring base pair, as shown in Fig. 7. The twist angle between the two base pairs is −7°. In previous studies (Valls *et al.*, 2007) this angle had been found to be around −25° for this virtual TA step.

It should be noted that the nature of the interactions which generate the coiled-coil geometry is different in the present case when compared with our previous studies of coiled coils (Campos *et al.*, 2005; De Luchi *et al.*, 2006). In the latter cases the coils are right-handed and kinks appear at the point of interaction between sticky ends of neighbouring duplexes, which have an identical structure at both sides of the duplex.

4. Discussion

Our results demonstrate a new mode of interaction of a minor-groove-binding drug with DNA. The charged ends of pentamidine detach from the DNA and are free to interact with neighbouring molecules in the crystal. Such interactions help to stabilize the coiled-coil structure of the stacked duplexes. In all previous studies with either pentamidine (Edwards *et al.*, 2003) or with other related drugs (Nguyen *et al.*, 2009) the drug remains tightly bound to the minor groove and is unable to bind to neighbouring molecules, whereas binding to an alternating all-AT sequence gives more freedom to the charged ends of the drug. In previous studies of drug interactions with the minor groove of d(CGCGAATTCGCG) the charged ends of the drug usually show hydrogen bonds to C·G base pairs, which may help to fix the drug inside the minor groove. It is obvious that the details of drug interaction depend on the DNA sequence.

The crystal lattice also has a strong influence. When drugs are associated with d(CGCGAATTCGCG) and related sequences, the oligonucleotide determines a rigid lattice through the interaction of the terminal C·G base pairs. As a result, the drug is fixed in space and cannot simultaneously interact with the minor groove and neighbouring molecules as observed in the present study. In fact, the crystal lattice we have found allows interaction of the drug with neighbouring duplexes. It is likely that other minor-groove-binding drugs, when placed in an appropriate environment, may also show interactions through their charged ends with neighbouring molecules (DNA, proteins *etc.*). It remains to be seen which of the two modes of interaction, either tight binding or end freedom, is favoured in a physiological environment. Other forms of interaction are possible. For example, in the case of transfer RNA it has been suggested (Sun & Zhang, 2008) that

the aromatic rings of pentamidine might be inserted into the stacked base pairs of the RNA.

The choice of DNA sequence is also important. Most previous studies have been carried out with the oligonucleotide duplex d(CGCGAATTCGCG)$_2$, as can be ascertained in the NDB. Work with this sequence has been very important to establish that in this case minor-groove-binding drugs are bound to the central GAATTC region. However, individual drugs may also bind to different AT-rich DNA sequences (Abu-Daya & Fox, 1997; Hampshire & Fox, 2008; Liu *et al.*, 2008). Further studies should be carried out using other sequences that occur more frequently in the genome, in particular longer all-AT sequences. There are only two previous cases where a TATATA hexamer sequence embedded in C·G base pairs has been used, in which netropsin and distamycin A were studied. In both cases the minor groove widens and accepts either two drug molecules (Mitra *et al.*, 1999) or one drug molecule and an extrahelical guanine (Abrescia, Malinina & Subirana, 1999). Recent work has also shown that the minor groove may simultaneously accommodate several drug molecules (Bazhulina *et al.*, 2009). All these observations differ from those that we present in this paper and confirm the need for further studies.

It remains to be shown whether the interaction that we have found may occur *in vivo*. The main feature of the structure presented here is the external position of the charged diamidine groups, which may thus interact with proteins and other molecules in the cell. When pentamidine interacts with proteins it is known that it may cross-link different regions of the molecule (Charpentier *et al.*, 2008). Pentamidine molecules bound to DNA in a nucleosome might also form cross-links between the two turns of DNA in regions which contain the appropriate DNA sequence. Such cross-links have been demonstrated in complexes with polyamide drugs (Suto *et al.*, 2003). Pentamidine is much smaller, but when placed in the minor groove of one turn of the nucleosome the drug could interact with phosphates in its other turn. This would require a small local distortion of about 2 Å so that the two turns are close enough. Such a distortion would alter the structure of the nucleosome and influence its biological function.

Another striking feature of our results is the different structure of the d(ATATATATAT)$_2$ duplex at its two ends. This peculiarity may arise from an optimization of the overall interactions in the crystal, such as end-to-end stacking and sideways drug–phosphate contacts. In any case our results confirm the versatility of the alternating AT sequence, which may be fully Watson–Crick (Yuan *et al.*, 1992; Abrescia, Malinina, Fernandez *et al.*, 1999), fully Hoogsteen (Abrescia *et al.*, 2002) or show a mixture of both kinds of base pairs as in the present case. Hoogsteen base pairs in alternating AT regions have also been postulated to occur when echinomycin is bound to DNA (Mendel & Dervan, 1987). Work with the ATAT tetramer also demonstrated a conformation different from that of the normal B form (Klug *et al.*, 1979). In duplexes which have all base pairs in the Watson–Crick conformation, the alternating AT sequence is also polymorphic (Yuan *et al.*, 1992), depending on the context of the sequence and the counterions present. Further work with different drugs and ionic environments is required in order to determine which structure they adopt when bound to different DNA sequences.

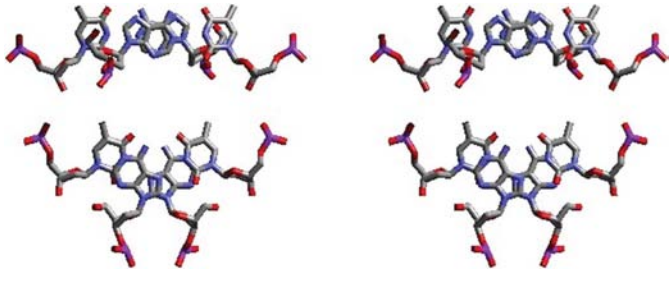

Figure 7
Stereoview of the stacking of the virtual TA base step between two oligonucleotide duplexes at the Watson–Crick end (top) and at the Hoogsteen end (bottom).

We are grateful to Drs. I. Fita and L. Malinina for discussion and advice. We thank Mr H. Millonig for help with the *Coot* program and the staff of the BM16 beamline at the ESRF for help in data collection. This work was supported by grant BFU2006-04035 from the Spanish Ministerio de Ciencia e Inovación.

References

Abrescia, N. G. A., Malinina, L., Fernandez, L., Huynh-Dinh, T., Neidle, S. & Subirana, J. A. (1999). *Nucleic Acids Res.* **27**, 1593–1599.
Abrescia, N. G. A., Malinina, L. & Subirana, J. A. (1999). *J. Mol. Biol.* **294**, 657–666.
Abrescia, N. G. A., Thompson, A., Huynh-Dinh, T. & Subirana, J. A. (2002). *Proc. Natl Acad. Sci. USA*, **99**, 2806–2811.
Abu-Daya, A. & Fox, K. R. (1997). *Nucleic Acids Res.* **25**, 4962–4969.
Baraldi, P. G., Bovero, A., Fruttarolo, F., Preti, D., Tabrizi, M. A., Pavani, M. G. & Romagnoli, R. (2004). *Med. Res. Rev.* **24**, 475–528.
Bazhulina, N. P., Nikitin, A. M., Rodin, S. A., Surovaya, A. N., Kravatsky, Y. V., Pismensky, V. F., Archipova, V. S., Martin, R. & Gursky, G. V. (2009). *J. Biomol. Struct. Dyn.* **26**, 701–718.
Campos, J. L., Urpí, L., Sanmartín, T., Gouyette, C. & Subirana, J. A. (2005). *Proc. Natl Acad. Sci. USA*, **102**, 3663–3666.
Chaires, J. B. (1997). *Biopolymers*, **44**, 201–215.
Charpentier, T. H., Wilder, P. T., Liriano, M. A., Varney, K. M., Pozharski, E., MacKerell, A. D. Jr, Coop, A., Toth, E. A. & Weber, D. J. (2008). *J. Mol. Biol.* **382**, 56–73.
Collaborative Computational Project, Number 4 (1994). *Acta Cryst.* D**50**, 760–763.
De Luchi, D., Tereshko, V., Gouyette, C. & Subirana, J. A. (2006). *Chembiochem*, **7**, 585–587.
Edwards, K. J., Jenkins, T. C. & Neidle, S. (2003). *Biochemistry*, **31**, 7104–7109.
Hampshire, A. J. & Fox, K. R. (2008). *Biochimie*, **90**, 988–998.
Klug, A., Jack, A., Viswamitra, M. A., Kennard, O., Shakked, Z. & Steitz, T. A. (1979). *J. Mol. Biol.* **131**, 669–680.
Lee, M. S., Johansen, L., Zhang, Y., Wilson, A., Keegan, M., Avery, W., Elliot, P., Borisy, A. A. & Keith, C. T. (2007). *Cancer Res.* **67**, 11359–11367.
Leonard, G. A., McAuley-Hecht, K., Brown, T. & Hunter, W. N. (1995). *Acta Cryst.* D**51**, 136–139.
Liu, Y., Collar, C. J., Kumar, A., Stephens, C. E., Boykin, D. W. & Wilson, W. D. (2008). *J. Phys. Chem. B*, **112**, 11809–11818.
Lu, X. J. & Olson, W. K. (2003). *Nucleic Acids Res.* **31**, 5108–5121.

Mendel, D. & Dervan, P. B. (1987). *Proc. Natl Acad. Sci. USA*, **84**, 910–914.
Mitra, S. N., Wahl, M. C. & Sundaralingam, M. (1999). *Acta Cryst.* D**55**, 602–609.
Murshudov, G. N., Vagin, A. A. & Dodson, E. J. (1997). *Acta Cryst.* D**53**, 240–255.
Navaza, J. (1994). *Acta Cryst.* A**50**, 157–163.
Nguyen, B., Lee, M. P. H., Hamelberg, D., Joubert, A., Bally, C., Brun, R., Neidle, S. & Wilson, W. D. (2002). *J. Am. Chem. Soc.* **124**, 13680–13681.
Nguyen, B., Neidle, S. & Wilson, W. D. (2009). *Acc. Chem. Res.* **42**, 11–21.
Otwinowski, Z. & Minor, W. (1997). *Methods Enzymol.* **276**, 307–326.
Pous, J., Urpí, L., Subirana, J. A., Gouyette, C., Navaza, J. & Campos, J. L. (2008). *J. Am. Chem. Soc.* **130**, 6755–6760.
Subirana, J. A. & Messeguer, X. (2008). *Gene*, **408**, 124–132.
Sun, T. & Zhang, Y. (2008). *Nucleic Acids Res.* **36**, 1654–1664.
Suto, R. K., Edayathumangalam, R. S., White, C. L., Melander, C., Gottesfeld, J. M., Dervan, P. B. & Luger, K. (2003). *J. Mol. Biol.* **326**, 371–380.
Tidwell, R. R. & Boykin, D. W. (2003). *Small Molecule DNA and RNA Binders*, edited by M. Demeunynck, C. Bailly & W. D. Wilson, pp. 414–460. Weinheim: Wiley–VCH.
Valls, N., Santaolalla, A., Campos, J. L. & Subirana, J. A. (2007). *J. Biomol. Struct. Dyn.* **24**, 547–551.
Wilson, W. D., Tanious, F. A., Mathis, A., Tevis, D., Hall, J. E. & Boykin, D. W. (2008). *Biochimie*, **90**, 999–1014.
Yuan, H., Quintana, J. & Dickerson, R. E. (1992). *Biochemistry*, **31**, 8009–8021.